MĀPAN-Journal of Metrology Society of India
https://doi.org/10.1007/s12647-024-00779-6

ORIGINAL PAPER

Modified Refractivity-Based Lifted Index Using Exact Formula for Lifted Condensation Level

F. K. Adejumobi[1], M. E. Sanyaolu[1], A. A. Willoughby[1] and O. F. Dairo[2]*

[1]Department of Physical Sciences, Faculty of Natural Sciences, Redeemer's University, Ede, Osun State, Nigeria

[2]Department of Electrical and Electronic Engineering, Faculty of Engineering, Redeemer's University, Ede, Osun State, Nigeria

Received: 26 January 2024 / Accepted: 05 October 2024

Abstract: Temperature is responsible for the rise of air parcels in the atmosphere, which in turn impairs the transmission of electromagnetic waves. Therefore, atmospheric stability is a function of the temperature of the rising and sinking air parcel with respect to the environmental air temperature at the lifted condensation level (LCL). Refractivity-based lifted index (RLI), a stability index model, uses an approximate LCL value. This study modifies the RLI using the exact formula of the LCL to obtain a precise modified refractivity-based lifted index (MRLI) model for the computation of refractivity-based atmospheric stability profiles. Two years (2020–2021) reanalysis data of atmospheric parameters (temperature, relative humidity and atmospheric pressure) were obtained from European Centre for Medium-Range Weather Forecasts (ECMWF) satellite for Lagos (6.6018° N, 3.3515° E), Abuja (9.0765° N, 7.3986° E) and Yola (9.2095° N, 12.4782° E) at 500–1000 hPa. RLI and MRLI were analysed at four synoptic hours (0, 6, 12, and 18 h) Local Time (LT). The trend shows that when RLI is negative, MRLI is negative; when RLI becomes less negative, MRLI is less negative, except in some cases where a significant amount of water vapour is observed at 500 hPa. Furthermore, a higher negative MRLI value indicates more environmental moisture and is supportive of convective activity, which implies an unstable atmosphere. MRLI has higher night-time (18–0 h LT) values compared to the daytime (6–12 h LT) due to low temperature and high humidity. Also, MRLI negative value decreases as the altitude increases with seasonal averages of − 97, − 86, and − 83 N-units over Lagos, Abuja, and Yola, respectively. A strong positive relationship was observed between MRLI and RLI, with correlation coefficients of 0.99999 for Lagos, 0.99823 for Abuja, and 0.99765 for Yola. MRLI attempts to lower the approximation error exhibited by RLI values for dry season months over Abuja and Yola.

Keywords: Radio refractivity profile; Air parcel; Atmospheric stability; Refractivity-based lifted index (RLI); Modified refractivity-based lifted index (MRLI)

1. Introduction

An extensive understanding of different meteorological parameter variations and formulations is crucial in solving problems related to atmospheric events under different climatic and environmental conditions. This is one of the fundamental requirements for proper radio transmission, weather forecasting and meteorological predictions because weather and climatic conditions are space- and time-varying unpredictably with instabilities across the globe. Instability is released when the air parcel is set in motion by a low-level moisture mechanism present in an unstable atmosphere. Thus, resulting in weather phenomena such as rain, thunderstorms, and convective weather are possible. Severe weather could be produced by moisture in the lower atmosphere, higher level divergence, and convergence [1].

Weather phenomena take place in the troposphere, which is the lowest part of the atmosphere that contains virtually all of the water vapour. Rigorous and appropriate weather forecasting models and formulations are needed to determine future climatic expectations and adequately understand the thermodynamic nature of our atmosphere. Having precise and accurate prediction formulations for

*Corresponding author, E-mail: dairof@run.edu.ng

Published online: 15 October 2024

atmospheric events can be very important for individuals, organisations, and national infrastructures. For instance, precise weather predictions on thunderstorms, cloud formations, severe turbulence, and other air hazards are essential to network connectivity and visibility. Using the conditional, latent, absolute, potential, or convective instability concepts, Peppler [2] stated that indices were created to examine the atmosphere's static stability level. The wind profile and potential disruption in the atmospheric boundary layer (ABL) can be determined from a stable atmosphere [3, 4]. However, due to turbulence and the positive vertical heat flux produced by ground stability or the water surface being warmer than the upper air, an unstable atmosphere may develop [5, 6].

Furthermore, studies [7–15] have shown that severe thunderstorms are often linked with high-intensity rainstorms, which naturally result in disaster and favour convection's triggering or initiation. Unstable weather like thunderstorms can also create ionospheric disturbances that affect radiofrequency communication. Several stability indices such as the Lifted Index (LI) [6, 16], Showalter Index [17], Modified Showalter Index [2, 18], and Adedokun Indices [19, 20], were developed. However, further research is needed to investigate and formulate an effective modified meteorological prediction and stability formula based on refractivity. Hence, it is a difficult challenge to enhance the prediction of thunderstorms, especially severe ones [21], which may help avoid or lessen damage. The thunderstorm rains are usually generated within the cumulonimbus cloud systems [22].

The initial temperature of the air parcel, T_p and the water vapour mixing ratio would define the vertical profile of the parcel temperature. Convection formation is more favourable by the buoyancy of an air parcel due to the warmer surrounding area. However, a cold environment will result in a stable air parcel, and the environment will be less supportive of convection occurrence. It should be noted that calculations of parcel temperature are essentially theoretical and only apply to environments for which measurement is possible. As a result, as pressure rises in a parcel until it is in equilibrium with the environment, it is possible to utilize that information to deduce the stability of the atmosphere by comparing the parcel's refractivity to that of the environment at various pressure levels [23, 24].

Several analytical and approximate expressions were proposed and formulated for this purpose, such as formulations for lifted condensation level LCL height and temperature. Lifted Condensation Level (LCL) represents the elevation (height) where the parcel of air would become saturated after undergoing adiabatic lifting [25]. A simplified approach for calculating an equivalent potential temperature still relevant in the tropics was described by Bolton's famous expressions [26]. In these formulations, absolute inaccuracy of several degrees can result due to a missing term in the derivation of the conventional formula. Similarly, Lawrence [27] used a very simple rule of thumb to approximate the conversion between relative humidity (RH) and temperature at the dew-point (t_d) for moist air (RH $>$ 50%). Another study [28] developed an empirical shortcut for calculating the pressure and temperature at the LCL.

More so, planning terrestrial radio links requires an understanding of surface refractivity as well as diurnal and seasonal variability. Hence, a higher refractivity seasonal variation is observed in the rainy season than in the dry [29]. Atmospheric stability can be described using different techniques and parameters such as Lapse Rate (Γ), measured in °C km^{-1} and defined as the rate at which the temperature changes with height. Dry Adiabatic Lapse Rate (DALR) is when unsaturated parcels cool at a rate of 9.8 °Ckm^{-1} while Moist Adiabatic Lapse Rate (MALR), for a saturated air parcel, is when $T = T_d$ it cools at the rate of 6 °C km^{-1}. Condensation occurs as saturated air rises, expands, and cools, releasing latent heat within the parcel. The cooling caused by expansion is compensated and reduced by the latent heat energy. Warm, moist air parcels have lower lapse rates than dry, adiabatic air parcels above the Lifted Condensation Level because the latent heat of vaporisation is released as the water vapour in the air parcel turns to liquid [23].

This study modifies the RLI using the exact formula of the LCL to obtain a precise model for the computation of a refractivity-based atmospheric stability profile known as the modified refractivity-based lifted index (MRLI). Hence, MRLI can provide a reference point for estimating or forecasting meteorological events to mitigate satellite communication network brownouts before extreme adverse weather situations. Satellite atmospheric parameter data over three geographical locations in Nigeria, namely Lagos (6.6018° N, 3.3515° E), Abuja (9.0765° N, 7.3986° E), and Yola (9.2095° N, 12.4782° E), were used to compute the MRLI. Similarly, this study uses the RLI formulation to simulate atmospheric stability based on the refractivity profile using the exact formula of the LCL. These were achieved by analysing the diurnal and seasonal influence of the exact equation of the LCL on the MRLI over the tropical study sites at four synoptic hours of the day (0, 6, 12, and 18 h LT). Also, the correlation between MRLI and RLI were estimated.

2. Radio Refractivity (N)

Radio refractivity, N, a derivative of the index of refraction [30, 31], is given by Eq. (1):

$$N = (n-1) \times 10^6 \tag{1}$$

Early studies [32, 33] showed radio refractivity as a mixture of dry air and water vapour at microwave frequencies. The radio refractivity, N, is a function of the local meteorological parameters and is formalised as (2) [34]

$$N = 77.6\frac{P}{T} - 5.6\frac{e}{P} + 3.75 \times 10^5 \frac{e}{T^2} \tag{2}$$

where, P (hPa) refers to the total atmospheric pressure, e (hPa) is the water vapour pressure and T (K) is the absolute air temperature. For temperatures in the range − 50 °C to + 40 °C. Equation (2) is summarised as

$$N = q_1\frac{P}{T} + q_2\frac{e}{T^2} \tag{3}$$

where $q_1 = 77.6$ K hPa^{-1} and $q_2 = 373000.0$ K^{2}hPa^{-1}. Refractivity is a dimensionless parameter (N is expressed in N-units). The first and second terms in the above refractivity equation of the atmosphere represent dry and wet terms, respectively [34–37].

The relationship between the relative humidity H (%) and water vapour pressure e is given by:

$$e = H\,e_s/100 \tag{4}$$

and,

$$e_s = a\ \exp\left[\frac{b\,t}{t+c}\right] \tag{5}$$

At temperature t (°C), e_s refers to the saturation vapour pressure (hPa) with the coefficients $a = 6.1121$, $b = 17.502$, and $c = 240.97$(being valid between − 20 to + 50 °C, with an accuracy of 0.20%) [33].

3. Lifted Index (LI)

LI is one of the common measures of atmospheric instability and is defined as the temperature difference between the environment, T_e (°C) and that of the air parcel, T_p (°C) at a particular pressure level in the lower atmosphere [6, 16, 23]. The surface air cools as it rises. It can sometimes cool more slowly than its surroundings, which leads to storm formation. As a result, atmospheric temperature decreases with altitude. The values of LI in Eq. (6) can be either negative or positive. The more negative LI is, the more unstable the air becomes, and the stronger the updrafts are likely to be with possibility of thunderstorms occurrence.

$$LI = T_e - T_p\ (^{\circ}C) \tag{6}$$

where T_e is the environmental temperature, and T_p is the air parcel temperature (Table 1).

4. Refractivity-Based Lifted Index (RLI)

Refractivity-based Lifted Index (RLI) was developed to provide results comparable to those of the lifted index usually generated from the radiosonde's relative humidity, pressure, and temperature profiles [23, 24].

The RLI equation is given as

$$RLI = q_1\frac{P\,LI}{T_pT_e} - q_2\frac{e}{T_e^2} \tag{7}$$

where $q_1 = 77.6$ K hPa^{-1} and $q_2 = 373000.0$ K^{2}hPa^{-1}. P is the pressure at 500 hPa, T_e refers to environmental temperature (K), T_p denotes the temperature of the air parcel (K) and e (hPa) denotes water vapour pressure of the environment. LI represents the lifted index $(T_e - T_p)$ [6].

5. Exact Formula of the Lifted Condensation Level (LCL)

Romps [25] successfully modified LCL formulation through optimized constant thermodynamic properties using the W_{-1} branch of Lambert W function to give exact formulations for LCL. As the air parcel undergoes adiabatic lifting to its LCL, the air parcel's potential temperature is perfectly conserved. This makes it possible to compare its temperature T and pressure p at the initial point to its temperature and pressure at the LCL. Exact equations of the LCL are given by

$$T_{LCL} = c\left[W_{-1}\left(RH_l^{1/a}ce^c\right)\right]^{-1}T \tag{8}$$

$$P_{LCL} = p\left(\frac{T_{LCL}}{T}\right)^{c_{pm}/R_m} \tag{9}$$

$$z_{LCL} = z + \frac{c_{pm}}{g}(T - T_{LCL}) \tag{10}$$

$$a = \frac{c_{pm}}{R_m} + \frac{c_{vl} - c_{pv}}{R_v} \tag{11}$$

$$b = -\frac{E_{0v} - (c_{vv} - c_{vl})\,T_{trip}}{R_vT} \tag{12}$$

$$c = {}^{b}/_{a} \tag{13}$$

RLI: Refractivity-Based Lifted Index.
MRLI: Modified Refractivity Based Lifted Index.
LCL: Lifted Condensation Level.
LI: Lifted Index.
RH: Relative Humidity (%).
T: Temperature (^{0} C or K).
P: Pressure (Pa).
Z: Height (m or Km).

Table 1 LI values interpretation [24]

Lifted Index	Stability
Over 0 (> 0)	Stable but weak convection possible for LI = 1–3 if strong lifting is present
0 to − 3	Marginally unstable
− 3 to − 6	Moderately unstable
− 6 to − 9	Very unstable
Below − 9 (< − 9)	Extremely unstable

W_{-1}: Lambert W function (the negative branch).

C: Specific heat capacity (J kg^{-1} K^{-1}).

RH_l: Parcel's relative humidity with respect to liquid water.

T_{LCL}: Temperature at the Lifted Condensation Level.

P_{LCL}: Pressure at the Lifted Condensation Level.

Z_{LCL}: Height of the parcel at the Lifted Condensation Level.

q_v: The mass fraction of water vapour present in the air parcel.

C_{pm}: The specific heat capacity at constant pressure (subscript m denoting the appropriate values for moist air).

C_{pa}: Dry air's specific heat capacity at constant pressure (J kg^{-1} K^{-1}).

C_{pv}: Specific heat capacity of water vapour at constant pressure (J kg^{-1} K^{-1}).

C_{vv}: Specific heat capacity of water vapour at constant volume (J kg^{-1} K^{-1}).

R_a: The dry air-specific gas constant (J kg^{-1} K^{-1}).

R_m: The air parcel's specific gas constant (J kg^{-1} K^{-1}).

R_v: Water vapour's specific gas constant (J kg^{-1} K^{-1}).

E_{0v}: Difference between the specific internal energy of liquid and water at the triple point.

T_d: Dew-point Temperature.

T_e: Temperature of the Environment (K).

T_p: Parcel Temperature (K).

θ_w: Wet-bulb Potential Temperature.

LT: Local Time.

6. Materials and Methods

6.1. Data Source

Hourly, daily and monthly temperature and relative humidity reanalysis datasets spanning 2020–2021 at 1000—500 hPa were used for this study. The tropical sites considered are Lagos (6.6018° N, 3.3515° E), Abuja (9.0765° N, 7.3986° E) and Yola (9.2095° N, 12.4782° E) in Nigeria. The datasets of these sites, at four synoptic hours (0, 6, 12, and 18 h) Local Time (LT), were obtained from from the archives of European Centre for Medium-Range Weather Forecasts, 2017 (ECMWF https://climate.copernicus.eu/). The fifth generation atmospheric re-analysis (ERA-5), which provides hourly meteorological data (relative humidity, pressure, and temperature), was required for characterise the propagation conditions. ERA-5 uses complex modelling and data assimilation technologies to turn massive volumes of historical data into global estimations. It gives an hourly worldwide value of atmospheric parameters with 137 vertical levels from the surface to 0.01 hPa and a horizontal resolution of 31 km (https://cds.climate.copernicus.eu/cdsapp#!/dataset/reanalysis-era5-complete?tab=form). The ERA5 data, downloaded in Network Common Data Form (NetCDF) format, were processed using the ferret and python packages [38].

6.2. Methodology

Daily data of four synoptic hours (0, 6, 12, and 18 h LT), which represent the diurnal variation, were averaged to provide monthly diurnal variation. Subsequently, they were averaged to create monthly data points, which were used to simulate refractivity-based lifted index (RLI) and modified refractivity-based lifted index.

6.3. Formulation of Modified Refractivity-Based Lifted Index

The modified refractivity-based lifted index (MRLI) was derived using the exact expression of the LCL. The improved model considers the saturation processes' temperature and pressure due to expansion and condensation caused by the dry lifting of an air parcel.

Considering the exact equation of the LCL, the temperature (T_{LCL}) and pressure (P_{LCL}) of the parcel are given by [24]

$$T_{LCL} = c\left[W_{-1}\left(RH_l^{1/a} c e^{c}\right)\right]^{-1} T \tag{14}$$

$$P_{LCL} = p\left(\frac{T_{LCL}}{T}\right)^{c_{pm}/R_m} \tag{15}$$

From Eq. (14), the initial air parcel temperature T is given by

$$T = \frac{T_{LCL}}{c\left[W_{-1}\left(RH_l^{1/a}ce^c\right)\right]^{-1}} \tag{16}$$

From Eq. (15), pressure P can also be expressed as

$$P_{LCL}\,T^{C_{pm}/R_m} = P\,T_{LCL}^{C_{pm}/R_m} \tag{17}$$

$$P = \frac{P_{LCL}\,T^{C_{pm}/R_m}}{T_{LCL}^{C_{pm}/R_m}} \tag{18}$$

Hence,

$$P = P_{LCL}\left(\frac{T}{T_{LCL}}\right)^{C_{pm}/R_m} \tag{19}$$

Substitute Eq. (16) into Eq. (19), we have

$$P = P_{LCL}\left(\frac{\frac{T_{LCL}}{c\left[W_{-1}\left(RH_l^{1/a}ce^c\right)\right]^{-1}}}{T_{LCL}}\right)^{C_{pm}/R_m} \tag{20}$$

$$P = P_{LCL}\left(\frac{T_{LCL}}{c\left[W_{-1}\left(RH_l^{1/a}ce^c\right)\right]^{-1}} \times \frac{1}{T_{LCL}}\right)^{C_{pm}/R_m} \tag{21}$$

$$P = P_{LCL}\left(\frac{1}{c\left[W_{-1}\left(RH_l^{1/a}ce^c\right)\right]^{-1}}\right)^{C_{pm}/R_m} \tag{22}$$

$$P = P_{LCL}\left(\frac{W_{-1}\left(RH_l^{1/a}ce^c\right)}{c}\right)^{C_{pm}/R_m} \tag{23}$$

Substituting the Eq. (23) into the RLI Eq. (7), gives

$$MRLI = q_1\frac{P_{LCL}\left(\frac{T}{T_{LCL}}\right)^{C_{pm}/R_m}LI}{T_pT_e} - q_2\frac{e}{T_e^2} \tag{24}$$

Thus, Eq. (24) is known as MRLI in terms of initial temperature T, temperature and pressure at the LCL (T_{LCL}, p_{LCL}).

where,

$$T_{LCL} = c\left[W_{-1}\left(RH_l^{1/a}ce^c\right)\right]^{-1}T \tag{25}$$

$$P_{LCL} = p\left(\frac{T_{LCL}}{T}\right)^{c_{pm}/R_m} \tag{26}$$

$$c_{pm} = (1-q_v)c_{pa} + q_vc_{pv} \tag{27}$$

$$R_m = (1-q_v)R_a + q_vR_v \tag{28}$$

$$C_{pv} = C_{vv} + R_v \tag{29}$$

$$C_{pa} = C_{va} + R_a \tag{30}$$

According to [28, 39], Eqs. (27 and 28) becomes

$$c_{pm}/R_m = 7/2 = 3.5 \tag{31}$$

where q_v is the mass fraction of water vapour present in the air parcel, R_m, the air parcel's specific gas constant, c_{pm} is the specific heat capacity at constant pressure with the subscript m denoting the appropriate values for moist air. R_a is the dry air specific gas constant, c_{pa} is dry air's specific heat capacity at constant pressure, R_v is the water vapour's specific gas constant and c_{pv} is the specific heat capacity of water vapour at constant pressure. LI is the lifted index and $q_1 = 77.6$ K hPa^{-1} and $q_2 = 373000.0$ K^2 hPa^{-1}.

$R_v = 461$ J kg^{-1} K.$^{-1}$.
$c_{vl} = 4119$ J kg^{-1} K.$^{-1}$.
$c_{vv} = 1418$ J kg^{-1} K.$^{-1}$.
$p_{trip} = 611.65$ Pa.
$T_{trip} = 273.16$ K.
$E_{0v} = 2.3740 \times 10^6$ J K.$^{-1}$.
$R_a = 287.04$ J kg^{-1} K.$^{-1}$.
$c_{va} = 719$ J kg^{-1} K.$^{-1}$.

Where,E_{0v} refers to the difference between the specific internal energy of liquid and water at the triple point [25].

7. Results and Analysis

Hourly, diurnal, and monthly values of meteorological parameters (temperature, pressure, and relative humidity) obtained for the years spanning 2020–2021 were used for the study. The data were collected over Lagos—a coastal area, Abuja—located in the tropical savannah, and Yola—a semi-arid region site. The study obtained values of saturation vapour pressure, e_s, water vapour partial pressure e, pressure P, and temperature T at the LCL using the reanalyses data of 1000 hPa level. Given the parcel- and environmental-temperature profiles, and humidity, the LI and the RLI were calculated using Eqs. (6) and (7), respectively. These values were determined for an air parcel originating at 1000 hPa. The LI and RLI values were then used to simulate the MRLI using Eq. 24 for a

parcel of air raised from 1000 to 500 hPa. T_{LCL} values of the exact formula of LCL were obtained using Wolfram Alpha Computational Intelligence software [40].

7.1. Diurnal Variation RLI over Lagos, Abuja and *Yola*

The diurnal variation of Refractivity-Based Lifted Index (RLI) for a parcel lifted from 1000 hPa level at 0, 6, 12, and 18 h LT over Lagos, Abuja and Yola is presented. Table 2 shows the typical distribution of RLI over Lagos at the four synoptic hours considered. Using Eq. (7), the determination of this index is possible with the availability of the refractivity profile and pressure, temperature and the water vapour mixing ratios at the surface or at the lower level where the air parcel is assumed to be originated. RLI in N-units ensures negative results whenever the LI is negative [23, 24]. At 500 hPa, the presence of a significant amount of water vapour can result in large positive RLI values even with smaller values of the LI, which indicates some form of stable atmosphere. Thus, for very large positive LI values, RLI gives positive values indicating the presence of a small amount of environmental moisture. Very high negative RLI values indicate support for convective precipitation and the presence of more moisture in the surrounding environment. On the other hand, since RLI was modelled to provide results comparable to the lifted index, RLI may be favourable for convective activities but if other conditions are not met as regards other atmospheric parameters, then no storms form. Thus, the fact that the lifted index is a theoretically derived parameter and not a measured quantity results in some sort of approximation

Table 2 Calculated daily refractivity based lifted index (RLI) for Lagos at four synoptic hours of the day (0, 6, 12, and 18 h LT)

	RLI (N-units)			
Day	0 h	6 h	12 h	18 h
1	− 120.69610	− 122.11407	− 118.34860	− 118.66255
2	− 108.48832	− 115.48003	− 124.12073	− 124.68236
3	− 121.24086	− 120.60081	− 122.90089	− 125.52610
4	− 127.51274	− 122.57273	− 121.50921	− 122.05620
5	− 116.43778	− 115.57586	− 114.24080	− 117.30777
6	− 121.42909	− 121.39022	− 121.83310	− 120.38405
7	− 117.47827	− 119.32615	− 119.49054	− 121.14728
8	− 122.13086	− 122.86967	− 118.84047	− 122.55687
9	− 117.26620	− 117.88796	− 116.43169	− 118.61570
10	− 116.52985	− 118.74396	− 119.21793	− 119.74080
11	− 116.58679	− 117.84564	− 115.37140	− 117.11486
12	− 118.36622	− 118.85692	− 115.19755	− 118.55174
13	− 117.94492	− 118.79639	− 119.72187	− 120.42460
14	− 117.42180	− 120.32878	− 118.59789	− 121.73850
15	− 120.94192	− 119.57950	− 118.67046	− 120.73426
16	− 125.60241	− 126.98400	− 121.29622	− 120.89098
17	− 123.27601	− 123.80415	− 118.51357	− 120.64438
18	− 117.78543	− 116.52386	− 111.41275	− 115.59827
19	− 116.12075	− 117.67881	− 116.44601	− 118.13403
20	− 116.68154	− 118.95969	− 117.62564	− 118.32688
21	− 120.83624	− 117.75813	− 112.84310	− 117.26448
22	− 117.97437	− 117.66712	− 112.68291	− 112.59508
23	− 116.94940	− 112.49426	− 114.55399	− 117.72439
24	− 118.00287	− 119.59049	− 116.44150	− 118.35419
25	− 120.88065	− 117.82342	− 120.01188	− 122.20691
26	− 119.45256	− 116.58832	− 117.61595	− 115.53832
27	− 118.59584	− 120.14071	− 115.94627	− 117.64268
28	− 120.71689	− 116.60688	− 114.59201	− 113.83098
29	− 114.74593	− 117.26549	− 116.72011	− 117.09604
30	− 115.38053	− 114.67082	− 113.98240	− 112.29807

error on the RLI values obtained. Applying the exact formula of the LCL on RLI minimises this error.

Figures 1a–d show the trend of the diurnal variation of Refractivity-Based Lifted Index at 1000 hPa for 0, 6, 12 and 18 h LT over Lagos, Abuja and Yola. Similarly, Fig. 2 shows the trend of the monthly RLI values over Lagos, Abuja and Yola at 1000 hPa.

From Fig. 1a–d, it was observed that the refractivity-based lifted index (RLI) is higher at midnight (0 h), mostly between − 108 and − 139 N-units with the exception of Yola having value as high as − 146 N-units. RLI value is between − 110 and − 129 N-units at 6 h of the day and − 100 to − 124 N-units at 12 h of the day for all the three locations except Abuja with the highest value of − 139 N-units at 6 h. The pattern of variation between these periods showed a slight drop in the RLI value from morning through the mid-day with Abuja and Yola mostly affected by this drop. In the evening period (18 h), the RLI values for all three locations oscillate between − 112 and − 138 N-units. Temperature is normally higher during the day. Thus, the variation of this RLI can probably be attributed to a fall in temperature value thereby making the

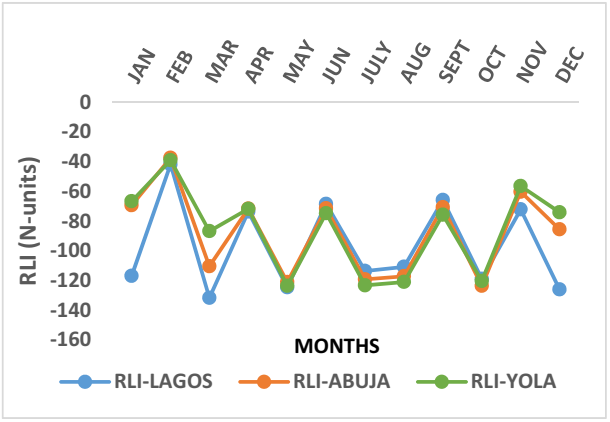

Fig. 2 Monthly variation of Refractivity-Based Lifted Index (RLI) at 1000 hPa over Lagos, Abuja and Yola

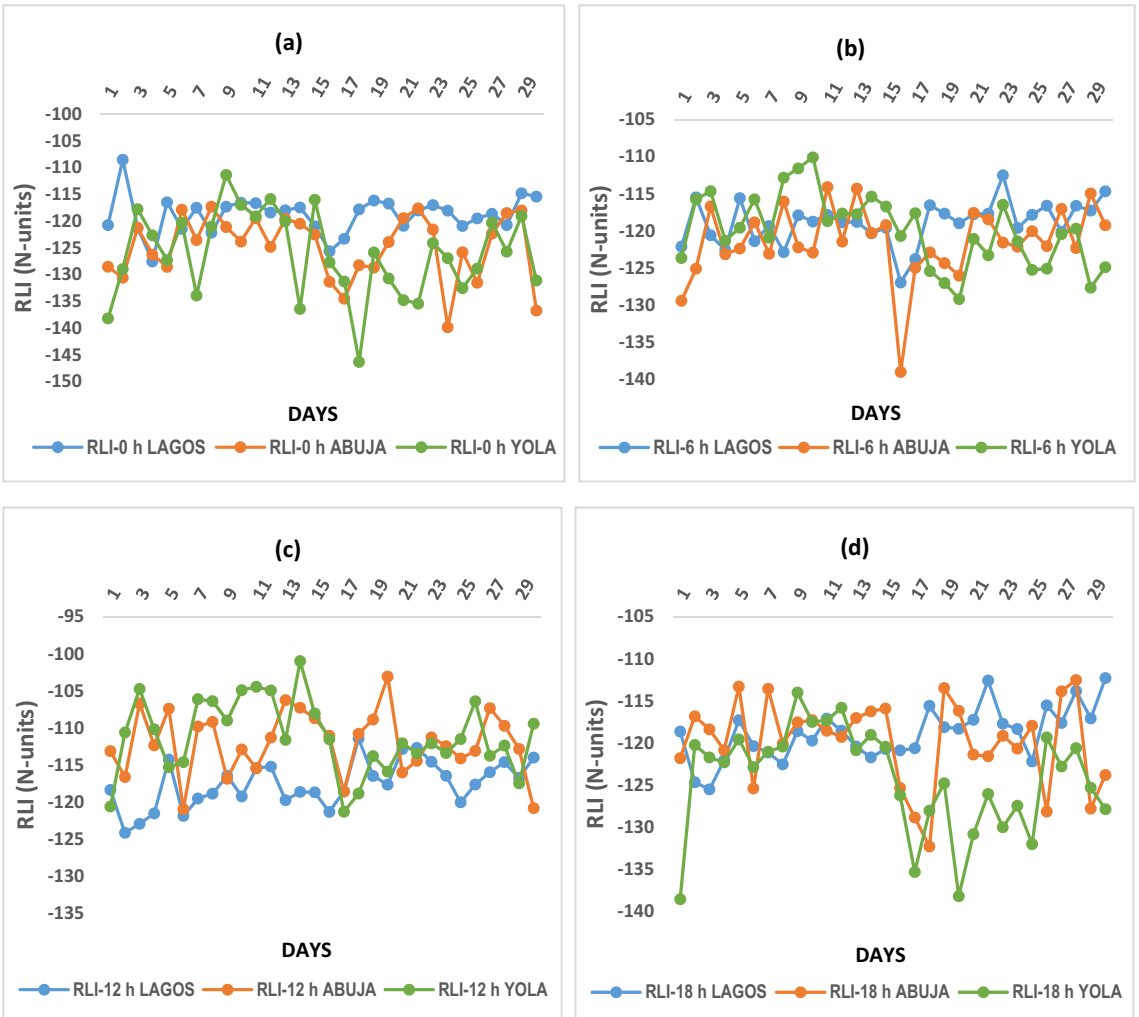

Fig. 1 Diurnal Variation of RLI for a parcel lifted at 1000 hPa for **a** 0 h, **b** 6 h, **c** 12 h, and **d** 18 h local time over Lagos, Abuja and Yola

environment more humid across each location as time shifts towards the night-time. The variation in the RLI value observed is linked to the stability of the atmosphere and moisture parameters [24].

7.2. Monthly Variation of RLI over Lagos, Abuja and *Yola*

This section presents the monthly variation of the Refractivity-Based Lifted Index at 1000 hPa over Lagos. Figure 2 reveals that RLI decreases as the altitude increases from November till around May, probably due to low environmental moisture content and high temperature alongside other atmospheric parameters. Hence, an increase in the water content increases the RLI as the altitude increases from June—October. It was observed that the average RLI value between March and November is − 98 N-units, − 96 N-units, and − 95 N-units, while − 95 N-units, − 64 N-units, and − 60 N-units between December and February for Yola for Lagos, Abuja, and Yola, respectively. This also shows an increase in negative RLI value as altitude increases during this period. Thus, RLI has a higher negative mean value in most of the wet months of the year in the three locations than in the dry months. This pattern can be attributed to the presence of high-water vapour content. Since a high negative RLI value can lead to the development of severe weather, it can be a threat to effective radio propagation. The pattern of RLI variation between December to February can be as a result of high temperatures with a very small environmental moisture of Abuja and Yola compared to Lagos which is close to the shore. Also, the yearly mean RLI value of − 97 N-units, − 88 N-units, and − 86 N-units follow the same trend for Lagos, Abuja, and Yola, respectively. Lagos has the highest negative RLI values in a year, followed by Abuja and Yola being the least. This formulation ensures that RLI is negative whenever the temperature-based lifted index (LI) is negative. Hence, the tendency of convective activity increases as RLI becomes more negative [23].

7.3. Daily Variation of Modified Refractivity-Based Lifted Index

The daily variation of MRLI for a parcel of air lifted from 1000 hPa level at 0, 6, 12, and 18 h LT over Lagos, Abuja and Yola is hereby presented. Unlike the dry component of the RLI that used temperature-based stability indices and pressure of the air parcel lifted, MRLI (N-units) model takes care of a situation where the parcel is expressed in terms of its pressure P at LCL and temperature T at LCL. MRLI was designed to give similar as RLI but with more accurate results. Hence, it ensures negative results whenever either temperature-based LI and the RLI is negative. The height difference between this parameter (LCL) and the LFC, which is the level of free convection is very important when determining convection initiation. MRLI combines the environmental water vapour information at the pressure at which the parcel was lifted (1000–500 hPa) with the atmospheric stability.

Furthermore, at 500 hPa, the presence of high-water vapour content can result in positive MRLI values just like the RLI even with a smaller value of the LI indicating some form of stable atmosphere. Hence, very high negative MRLI values indicate support for a convective weather condition with the presence of more moisture in the surrounding environment, which may have an undesirable effect on the performance of the radio communication link.

From Figs. 3a–d, it was observed that the MRLI is higher at midnight (0 h LT) with values mostly between -108 and -139 N-units except for Yola with the highest value of -146 N-units. At 6 h LT, MRLI values are between the range of -109.6 and -129 N-units for all three locations except Abuja having the highest value of -139 N-units. Also, at 12 h LT, all three locations have a value range of -98 to -124 N-units. The pattern of variation between these periods also showed a slight drop in the MRLI value between 6 and 12 h mid-day. Abuja and Yola were mostly affected by the drop in the MRLI values. At the evening hour of the day (18 h LT), the negative MRLI value for all three locations begins to rise from -112 to -137 N-units. Temperature is normally higher than night-time during the day, which can be as high as 31, 37, and 41 °C for Lagos, Abuja and Yola, respectively. Thus, this observation of unstable values that rise and fall can probably be attributed to a drop in the temperature resulting in high humidity and or moisture content across each location as time swings towards the evening or night-time [41, 42].

7.4. Monthly Variation of MRLI

Refractivity-Based Lifted Index (RLI) at 1000 hPa over Lagos, Abuja and Yola is presented.

Figure 4 shows that the modified refractivity-based lifted index (MRLI) decreases as altitude increases from November to May, possibly, as a result of low environmental moisture along with other varying atmospheric parameters. Hence, as the humidity and moisture content begin to increase, MRLI increases as altitude increases from June to October. More so, it was observed that the average negative MRLI value between March and November is − 97.8 N-units for Lagos, − 95 N-units for Abuja, and − 92.8 N-units for Yola. On the other hand, the average MRLI value between December and February is − 95 N-units, − 58.8 N-units, and − 52.9 N-units for Lagos, Abuja, and Yola, respectively. The pattern of MRLI variation from December to February can be attributed to

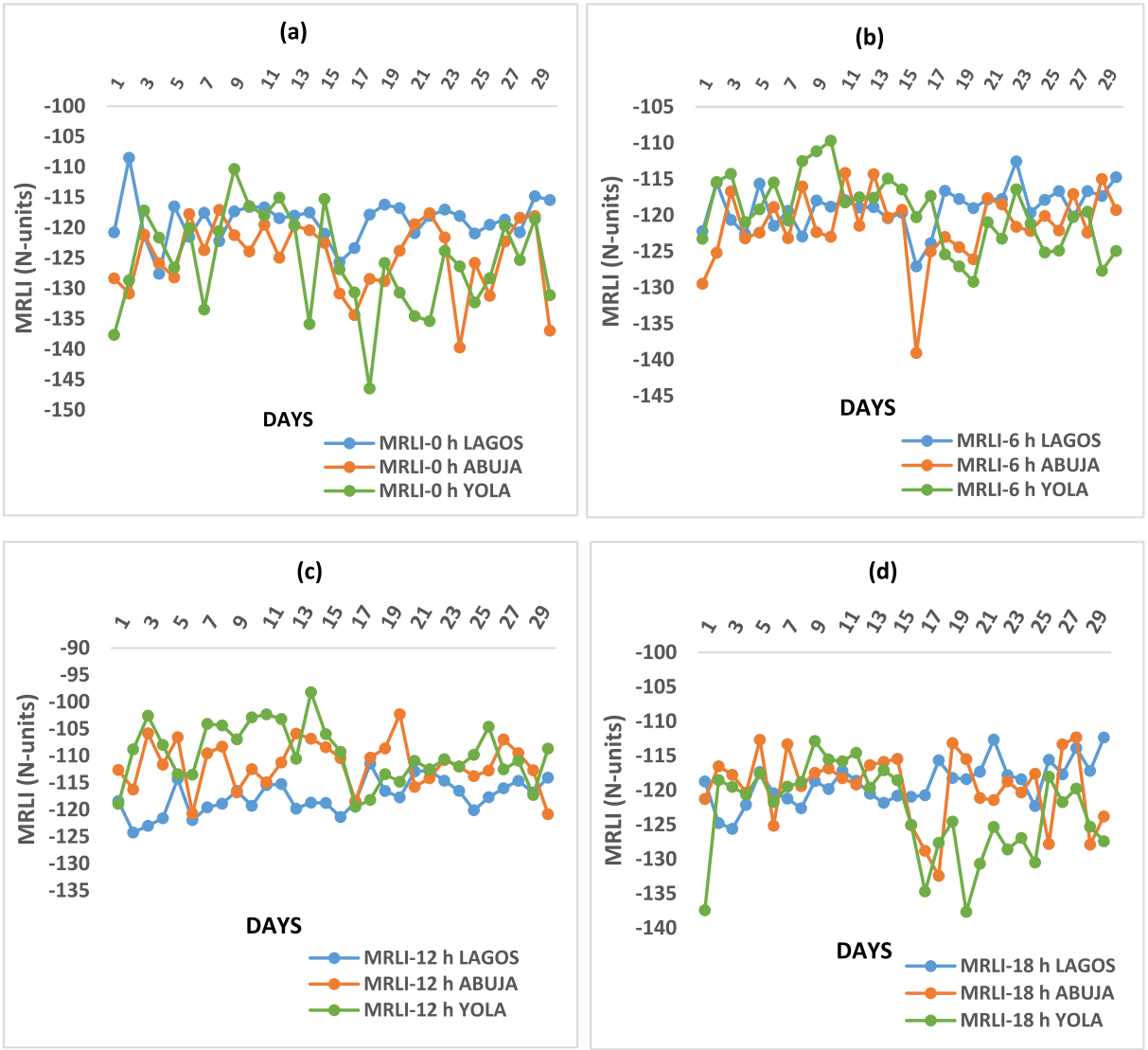

Fig. 3 Daily Variation of MRLI for a parcel lifted to 500 hPa for **a** 0 h, **b** 6 h, **c** 12 h, and **d** 18 h local time over Lagos, Abuja and Yola

high temperatures and low environmental moisture content over Abuja and Yola compared to Lagos which is close to the coastline. Thus, the yearly average MRLI values of − 97 N-units, − 86 N-units, and − 83 N-units for Lagos, Abuja, and Yola, respectively, show that the MRLI value decreases as the latitude increases. Lagos has the highest monthly negative MRLI values in a year, followed by Abuja and Yola being the least.

7.5. Seasonal Variation of the RLI with MRLI and Estimation of Correlation Between MRLI and RLI

The seasonal variation shows the correlation between MRLI and RLI. Figures 5a–c represent the seasonal variation of the RLI and MRLI for Lagos, Abuja and Yola. It

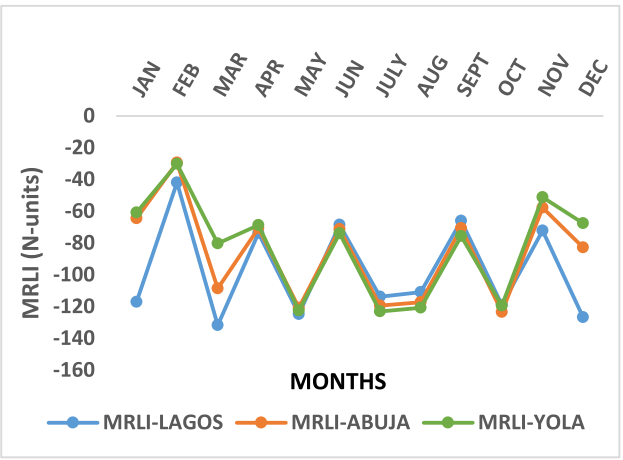

Fig. 4 Monthly variation of Refractivity-Based Lifted Index (RLI) at 1000 hPa over Lagos, Abuja and Yola

was observed that a high negative RLI value results in a high negative MRLI value with better accuracy than RLI northward in the Savannah and Sahel climates over Abuja and Yola, respectively.

MRLI values are very close to RLI from January to December with a correlation coefficient of 0.99999 and a standard error (SE) of approximately 0.14. This is obvious in Fig. 5a showing an almost perfectly fit plot between RLI and MRLI. The correlation coefficient can fall within the range of -1– $+$ 1.0 (where a correlation of $-$ 1.0 represents a perfect negative correlation, while a correlation of 1.0 shows a perfect positive correlation). The closeness in their values for Lagos from January to December can be attributed to its tropical climate with high humidity year-round and little interruption in the convective activity between July and August.

In addition, Fig. 5b shows this variation increases with latitude for dry periods across the three locations. This is attributable to the expression of the dry component of the RLI model in terms of the temperature-based lifted index (LI) for an air parcel lifted from 1000 to 500 hPa, without considering other events from the surface to when the air parcel is forced into the vertical lifting. From Fig. 5b, the variation of the RLI and MRLI gives a correlation coefficient of 0.99823 with a standard error (SE) of 1.8 for Abuja.

Figure 5c shows some variation between the RLI and MRLI values from January to March and November to December for Yola. This variation is a bit higher compared to Lagos and Abuja. Similarly, Fig. 5c shows that RLI values exhibit more deviation in the dry seasons than the wet seasons with a correlation coefficient of 0.99765 and SE of 2.08. There is also the existence of a strong relationship between the RLI and MRLI. Hence, MRLI attempts to lower the approximation error exhibited by RLI values for dry season months over Abuja and Yola.

Thus, the ability of the MRLI model to integrate the exact formula of the LCL (P_{LCL} and T_{LCL}) alongside the temperature-based lifted index (LI) and other meteorological parameter variations from where the parcel is lifted to

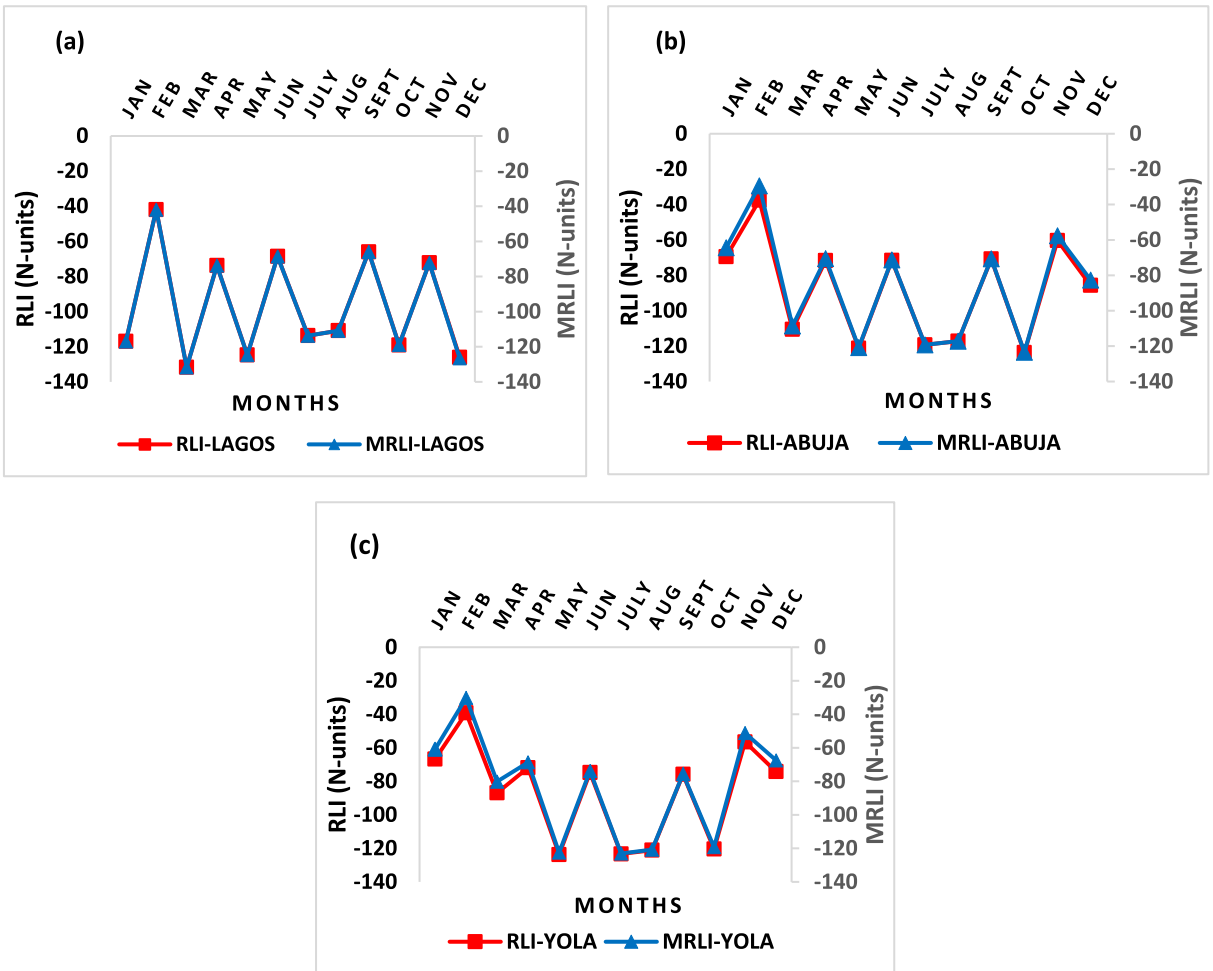

Fig. 5 Seasonal Variation of the RLI with MRLI for **a** Lagos, **b** Abuja and **c** Yola

500 hPa level makes it a more accurate adaptable model for estimating, forecasting weather conditions and for predicting the performance of terrestrial radio links for both the dry and wet seasons of all the three geographical locations.

8. Conclusion

The refractivity-based lifted index (RLI) has been modified using the exact formula of the lifted condensation level (LCL). This study has shown firstly that the pattern of variation of the RLI and MRLI showed that MRLI is negative whenever RLI is negative. Also, MRLI returns less negative when RLI is less negative except in some situations at 500 hPa where a significant amount of water vapour is observed. In this case, when RLI is negative, MRLI remains a bit more negative for Lagos, and less negative for Abuja and Yola.

Secondly, as the MRLI value decreases from 0 to − 30 N-units and below, the probability of convective activity also increases. This shows that more negative MRLI is indicative of more environmental moisture in addition to being supportive of convective activity. Also, MRLI has higher negative values from dusk to midnight (18–0 h LT) compared to daytime (6–12 h LT) due to low temperature and high humidity. MRLI negative value decreases as latitude increases across the three locations with seasonal average MRLI value of − 97 N-units over Lagos, − 86 N-units at Abuja, and − 83 N-units at Yola. Temperature variations with environmental moisture content have a great impact on the MRLI model performance over Abuja and Yola, especially during the dry season months of December–February, with values of − 58.8 N-units and − 52.9 N-units, respectively, compared to − 95 N-units for Abuja and − 92.8 N-units for Yola between March–November. Lagos showed a minimal MRLI difference, − 97.8 N-units for March–November and − 95 N-units for December–February.

Finally, the MRLI model displayed a strong positive systematic relationship with the RLI model by giving similar results as the RLI with a correlation coefficient of 0.99999 for Lagos, 0.99823 for Abuja and 0.99765 for Yola. MRLI attempts to lower the approximation error exhibited by RLI values for dry season months over Abuja and Yola.

Acknowledgements The authors thank Redeemer's University for the privilege given and the anonymous reviewers.

Declarations

Competing Interests The authors declare no known competing financial interests or personal relationships that could have appeared to influence the work reported in this paper.

References

[1] R.G. Beebe and F.C. Bates, A mechanism for assisting in the release of convective instability. Monthly Weather Review, *83* (1955) 1–10.
[2] R. A. Peppler, A review of static stability indices and related thermodynamic parameters, MP-104, ISWS Miscellaneous Publication, (1988)
[3] B. Lange, S. Larsen, J. Hojstrup and R. Barthelmie, The influence of thermal effects on the wind speed profile of the coastal. Boundary-Layer Meteorology, *112* (2004) 587–617.
[4] A. Pea and A.N. Hahmann, Atmospheric stability and turbulence fluxes at horns rev-an inter-comparison of sonic, bulk and WRF model data. Wind Energy, *15* (2012) 717–731.
[5] A.S. Monin and A.M. Obukhov, Basic laws of turbulent mixing in the surface layer of the atmosphere. Trudy Geofiz Instituta Akademii Nauk SSSR., *24* (1954) 163–187.
[6] J.G. Galway, The lifted index as a predictor of latent instability. Bulletin of the American Meteorological Society, *37* (1956) 528–529.
[7] R. Banta, Meteorological Monographs., American Meteorological Society, (1990)
[8] C. Barthlott, U. Corsmeier, C. Meißner, F. Braun and C. Kottmeier, The influence of mesoscale circulation systems on triggering convective cells over complex terrain. Atmospheric Research, *81* (2006) 150–175.
[9] M. Feldmann, A. Hering, M. Gabella and A. Berne, Hailstorms and rainstorms versus supercells—a regional analysis of convective storm types in the Alpine region. Npj Climate and Atmospheric Science, *6*(1) (2023) 19. https://doi.org/10.1038/s41612-023-00352-z.
[10] R. Kaltenboeck and M. Steinheimer, Radar-based severe storm climatology for Austrian complex orography related to vertical wind shear and atmospheric instability. Atmospheric Research, *158* (2015) 216–230.
[11] B. Katona and P. Markowski, Assessing the influence of complex terrain on severe convective environments in northeastern Alabama. Weather Forecast, *36* (2021) 1003–1029.
[12] M. Kunz, The skill of convective parameters and indices to predict isolated and severe thunderstorms, Natural Hazards and Earth. System, *7* (2007) 327–342. https://doi.org/10.5194/nhess-7-327-2007.
[13] H. Orville, A numerical study of the initiation of cumulus clouds over mountainous terrain. Journal of Atmospheric Science, *22* (1965) 684–699.
[14] M. Taszarek, J. Allen, T. Púčik, P. Groenemeijer, B. Czernecki, L. Kolendowicz, K. Lagouvardos, V. Kotroni and W. Schulz, A climatology of thunderstorms across Europe from a synthesis of multiple data sources. Journal of Climate, *32* (2019) 1813–1837.
[15] L. Zhu, L. Bai, G. Chen, Y.Q. Sun and Z. Meng, Convection initiation associated with ambient winds and local circulations over a tropical island in South China. Geophysical Research Letters, *48* (2021) e2021GL094382. https://doi.org/10.1029/2021GL094382.
[16] A. F. Sadowski and R. E. Rieck, Stability indices, TPB-207, NOAA NWS, (1977)
[17] A.K. Showalter, A stability index for thunderstorm forecasting. Bulletin of the American Meteorological Society, *34* (1953) 250–252.

[18] R.C. Curtis and H.A. Panofsky, The relation between large-scale vertical motion and weather in summer. Bulletin of the American Meteorological Society, *39* (1958) 521–531.
[19] J.A. Adedokun, Potential instability and precipitation occurrence within an inter-tropical discontinuity environment. Archives for Meteorology Geophysics and Bioclimatology Series B Theoretical and Applied Climatology, *30*(1–2) (1981) 69–86.
[20] J.A. Adedokun, On an instability index relevant to precipitation forecasting in West africa. Archives for Meteorology Geophysics and Bioclimatology Series B Theoretical and Applied Climatology, *31*(3) (1982) 221–230.
[21] E.M. Murillo, C.R. Homeyer and J.T. Allen, A 23-year severe hail climatology using gridrad mesh observations. Mon. Weather Rev., *149* (2021) 945–958.
[22] A. Hassen, Indicators for the signal Degradation and Optimization of Automotive Radar Sensors under Adverse Weather Conditions, PhD Dissertation submitted to Elekrotechnik and Informations Technik der Technishen, University of Darmstadt, (2006)
[23] D. Jagadheesha, B. Manikiam, N. Sharma and P.K. Pal, Atmospheric stability index using radio occultation refractivity profiles. J Earth Syst Sci, *120* (2011) 311–319.
[24] S.E. Falodun, J.S. Ojo and A.I. Kareem, The study of atmospheric stability using radio refractivity profiles over a tropical climate in Nigeria. MAPAN-J. Meteorol. Soc. India, *36* (2021) 751–762.
[25] D.M. Romps, Exact expression for the lifting condensation level. Journal of the Atmospheric Sciences, *74* (2017) 3891–3900.
[26] D. Bolton, The computation of equivalent potential temperature. Monthly Weather Review, *108* (1980) 1046–1053.
[27] M.G. Lawrence, The relationship between relative humidity and the dewpoint temperature in moist air: A simple conversion and applications. Bulletin of the American Meteorological Society, *86* (2005) 225–233.
[28] S.L. Barnes, An empirical shortcut to the calculation of temperature and pressure at the lifted condensation level. Journal of Applied Meteorology and Climatology, *7* (1968) 511–511.
[29] B.G. Ayantunji, P.N. Okeke and J.O. Urama, Seasonal variation of surface refractivity over Nigeria. Advances in Space Research, *48* (2011) 2023–2027.
[30] E.L. Smith and S. Weintraub, The Constants in the Equation for Atmospheric Refractive Index at Radio Frequencies. Proc. IRE, *41* (1953) 1035–1037.
[31] O.F. Dairo and L.B. Kolawole, Radio refractivity gradients in the lowest 100 m of the atmosphere over lagos, Nigeria in the rainy-harmattan transition phase. J. Atmosp. Solar-Terrest. Phys., *167* (2018) 169–176. https://doi.org/10.1016/j.jastp.2017.12.001.
[32] B. R. Bean and E. J. Dutton, Radio meteorology, US department of commerce, National Bureau of standards monograph 92, (1966)
[33] A.A. Willoughby, T.O. Aro and I.E. Owolabi, Seasonal variations of radio refractivity gradients in Nigeria. J. Atmos. Solar-Terres. Phys., *64* (2002) 417–425.
[34] ITU-R P.453–12, *The Radio Refractive Index; its Formula and Refractivity Data, Tech. rep., ITU*. Geneva, Switzerland, 2016.
[35] E. Forootan, M. Dehvari, S. Farzaneh and S. Karimi, Improving the Wet Refractivity Estimation Using the Extremely Learning Machine (ELM) Technique. Atmosphere, *14* (2023) 112. https://doi.org/10.3390/atmos14010112.
[36] S. Kim and S.-W. Kim, Estimation of Atmospheric Radio Refraction Errors for Ground Stations. IEEE Transactions on Aerospace and Electronic Systems (2023). https://doi.org/10.1109/TAES.2023.3335913.
[37] B. Sánchez-Rama, R.N. López, V.S. Del Río and T. Darlington, Radar-Based Refractivity Maps Using Geostatistical Interpolation. IEEE Geoscience and Remote Sensing Letters (2023). https://doi.org/10.1109/LGRS.2023.3328499.
[38] D. Tetzner, E. Thomas and C. Allen, A validation of ERA5 reanalysis data in the Southern Antarctic Peninsula—Ellsworth Land Region, and its implications for ice core studies. Geosciences, *9* (2019) 1–17. https://doi.org/10.3390/geosciences9070289.
[39] K. Supawat, T. Thanaset, S. Samran and T. Chanchai, Numerical method of microwave heating to modified for lifting condensation level of clouds formation, Proceedings of the World Congress on Engineering 2017 Vol I WCE 2017, London, UK, (2017)
[40] Wolfram Research, Inc., (2024). Wolfram Alpha Computational Intelligence Software. https://www.wolframalpha.com/
[41] A. Ahlawat, S.K. Mishra, M.V.S.N. Prasad, C. Sharma, V. Goel, S.R. Radhakrishnan and B. Gupta, Vertical profiling of radio refractivity and associated parameters using tethered balloon over New Delhi. MAPAN-J. Metrol. Soc India, *34* (2019) 479–485.
[42] E.E. Mahmoud, Realization of relative humidity scale from 10% to 98% at 25°C. MAPAN-J. Metrol. Soc India, *24*(4) (2009) 241–245.